Journal of Materials Chemistry B

Accepted Manuscript

ROYAL SOCIETY OF CHEMISTRY

www.rsc.org/materialsB

Journal of Materials Chemistry B RSCPublishing

ARTICLE

Porous PdO Microrods-based Electrochemical Sensor for Nanomolar-Level Cu^{2+} Released from Cells

Cite this: DOI: 10.1039/x0xx00000x

Received 00th July 2014,
Accepted 00th July 2014

DOI: 10.1039/x0xx00000x

www.rsc.org/

Xia Cao, [a,c*] *Yu Han,* [a,b] *Caizhen Gao,* [a,b] *Ying Xu,* [a,b] *Xiaomin Huang,* [a,b] *Magnus.Willander* [a], *and Ning Wang* [b]*

Highly porous PdO microrods (PoPdOMR) with well-defined morphology, large surface area and active sites were synthesized via a facile wet chemical method for the first time. A sensitive and selective electrochemical sensor was thus developed by using the PoPdOMR as sensing platform. The PoPdOMR modified sensor exhibited a response time less than 8 s, a linear range between 1.0×10^{-9} to 8.0×10^{-5} mM, and a sensitivity up to 112 $\mu A \bullet \mu M^{-1} \bullet cm^{-2}$ for the determination of Cu^{2+}. A sound sensing selectivity towards Cu^{2+} in the presence of interfering ions was also observed. On the basis of this sensor, the trace amount of Cu^{2+} released from Raw 264.7 cells was successfully recorded, which makes the PoPdOMR electrocatalyst promising for the development of effective electrochemical sensors for a wide range of potential applications in bioanalysis and environmental chemistry.

1. Introduction

Cu^{2+} is an essential metal ion for biological functions. However, at elevated concentrations, it is highly toxic to organisms such as algae, fungi, and many bacteria. As for humans, such ions may adversely affect the gastrointestinal, hepatic, and renal systems.[1-4] Therefore, detection and measurement of copper ions have become increasingly important to take advantage of its beneficial aspects while avoiding its toxic effects.[5] Up to date, various strategies and technologies have been developed to detect Cu^{2+}, including atomic absorption spectrometry, UV-vis spectra, fluorescence anisotropy assay,[6, 7] inductively coupled plasma atomic emission spectrometry (ICP-AES).[8-10] Among the variety of new analytical tools, electrochemical sensor has been recognized as one of the most sensitive methods for trace analysis of heavy metals.[1, 11-14] Compared to its spectroscopic competitors such as atomic absorption and atomic emission spectroscopy, electrochemical sensor has the advantage of on-site environmental monitoring due to its favorable portability, suitability for automation, short analysis time, low power consumption, and inexpensive equipment.[15, 16 17]

Nanomaterials of various shapes, sizes, and compositions have found broad applications in many kinds of analytical methods.[18] These materials often exhibit unique chemical, physical, and electronic properties that cannot be achieved by their bulk counterparts, which make them suitable for construction of electrochemical sensors and biosensors.[19-21] It should be noted that these sensors, like many other well-established electrodes for stripping voltammetry, are still subjected to interference from other heavy metal ions such as the formation of intermetallic compounds and peak overlapping problems, which are specific and relate to the nature of the stripping measurement.[22, 23] Thus, new electrode materials for stripping analysis are still highly desired to meet the growing demands for on-site environmental monitoring of trace heavy metal ions with high selectivity.[21, 24]

Palladium nanomaterials have been widely used as catalysts for a variety of research fields ranging from organic synthesis and fuel cells to environmental protection.[25, 26] However, in comparison with the wide study of Pd metal nanoparticles, PdO was generally used as a catalyst support in the past and has rarely been considered to be electrochemically active.[27] As a result, researches on the synthesis and electrochemical study of its oxide counterpart (PdO) are quite rare.[28-31] However, from a positive point of view, the Pd-PdO double-phase boundary can serve as highly conductive layer promoting the heterogeneous oxidation or reduction of the adsorbed agents, and the converted Pd ions can be continuously recovered by electrochemical oxidation or reduction.[32] As the electron transport can be readily tuned by the porous structure, the directional matter flow and consequential vacancy accumulation may further provide possibilities for chemists to design and synthesize new electrocatalysts for various electrochemical applications. In all of these areas, tunable size, shape, composition with fast, high-yield, and controllable synthesis are highly desirable and still remains critically challenging issues.[3, 33, 34]

In this paper, the porous PdO microrods (PoPdOMR) were prepared by a facile wet chemical route, a highly sensitive and selective Cu^{2+} sensor based on the PdO microrods was developed which is inspired by excellent catalytic activity of

PdO in copper electroplating. The proposed method could detect Cu^{2+} with a detection limit down to 1nM. We also demonstrate that this sensor could successfully detect the trace amount of Cu^{2+} released by cells. The superior catalytic activity and selectivity make this type of material very promising for applications in environmental and biological sciences.

2. Experimental Section

2.1 Reagents and Materials.

Palladium (II) acetate was purchased from Sigma-Aldrich and used as received. All other reagents, unless otherwise stated, were of analytical grade and were purchased from Sinopharm Chemical Reagent Beijing Co. Ltd and used without further purification. All other reagents, unless otherwise stated, were of analytical grade and were used without further purification. Phosphate-buffered saline (PBS, 50 mM, pH 7.4) containing 1% (w/v). Deionized and distilled water was used throughout the study.

2.2 Synthesis of the Porous PdO Microrods.

Briefly, 20 mL of a freshly prepared solution containing 10 mL of acetate, 10 mL of dimethyl sulfoxide, and 10 mg of palladium (II) acetate was quickly mixed with 10 mL of ethylene glycol. The mixture was then placed in a 50 mL beaker, heated to 130 ^{o}C and kept at this temperature for 3 hours. After cooling down to room temperature, the brown powders were collected by centrifuge, washed with pure water and methanol several times, and then dried in vacuum at 60 ^{o}C for further characterizations. Mesoporous PdO microrods were thus obtained by thermally treating the as-synthesized brown powders in air at 400 ^{o}C for 1 h.

2.3 Fabrication of Porous PdO Microrods Modified Electrodes.

To modify the electrode surface, an aliquot of 5 μL of 5 mg/mL PoPdOMR suspension in ethanol was dropped onto a GCE electrode surface (d = 3 mm). After drying in air, 5 μL of Nafion solution (1 wt% in ethanol) was cast on the layer of porous PdO microrods in order to entrap porous PdO microrods. The as prepared porous PdO microrods modified electrodes (PoPdOMRE) were immersed in water for 1 h to wet the Nafion layer thoroughly before use. In addition, the bulk PdO modified electrodes were made by the same way and used for comparison.

2.4 Electrochemical Cu^{2+} Sensor.

Scheme 1 shows a schematic illustration of the stepwise procedure and reaction mechanism of the Cu^{2+} sensor. The PoPdOMR, as the signal transduction, were coupled with Nafion to form the nanocomposite film on a glassy carbon electrode. With the reduction of PdO, more active sites on the electrode were created. The electrocatalytic response of Cu^{2+} was dramatically increased owing to the formed conductive properties of the nanocomplex. Enhanced signal amplification is expected from the catalytic activity of the porous PdO microrods toward the reduction of Cu^{2+}.

2.5 Detection of Cu^{2+} Released from RAW 264.7 Cells.

Raw 264.7 cells (obtained from Sigma) were grown in 5% CO_2 in 75 cm^2 flasks containing Dulbecco's modified Eagle's medium with 1% antibiotics and 10% (v/v) fetal bovine serum (FBS) at 37 °C. After growing to 90% confluence, the cells were collected by centrifugation and washed with PBS three times. The number of the cells was counted by a hemocytometer. During the test, a pellet that contained 2×10^6 cells was resuspended into 20 mL of PBS (0.1 M, pH = 7.4) and the mixture was saturated with N_2. A potential of 300 mV (vs SCE) was applied to the PdO microrods modified electrode. A 0.3 μM solution of 3-[(3-Cholamidopropyl) dimethylammonio]-1-propanesulfonate (CHAPS, 97%, Aldrich) was added into the solution after a steady background noise was obtained.

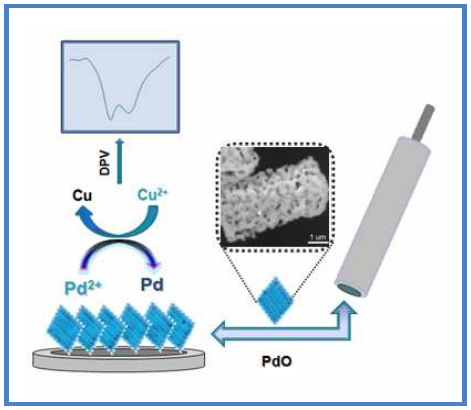

Scheme1. Schematic routine of the electrochemical sensing platform for Cu^{2+} ion.

2.6 Characterization Techniques.

The as-synthesized porous PdO microrods were characterized by using a Hitachi S4800 cold field emission scanning electron microscope (CFE-SEM) and transmission electron microscope (TEM). X-ray powder diffraction (XRD) patterns of the products were collected by a Rigaku X-ray diffractometer (Rigaku Goniometer PMG-A2, CN2155D2, wavelength = 0.15147 nm) with Cu Kα radiation. All electrochemical measurements were performed at room temperatures under air or nitrogen saturated PBS (pH = 7.4) solution on a CHI 660C electrochemical station, using a single compartment, three-electrode cell. Electrode potentials were measured with respect to an aqueous saturated calomel electrode (SCE). A Pt wire was used as the counter electrode. The data of condition, optimization, and calibration curve were the average of three measurements.

3. Results and discussion

Scanning electron microscopy (SEM) images (Figures 1A-B) show that the PoPdOMR are grown with high uniformity at a large scale. The average edge length of these microrods was 400 nm and elongated along one of the axes to form hexagonal bars/rods. The aspect ratios (length to width) are larger than six, and the hexagonal bars are enclosed by well-organized facets. More interestingly, the as prepared PdO microrods are made of loosely interconnected PdO nanochains with a low packing density, which presents typical porous nature. XRD result (Figure 1C) shows that the porous microcrystal is pure phase PdO with a typical tetragonal structure. TEM results give further structural information of the porous PdO microrods (Figures 1D-E). The average size of the interconnected chains is about 30-50 nm. The high-resolution TEM (HRTEM) image

(Figure 1F) indicates the porous microrods are well crystallized with local orientation.

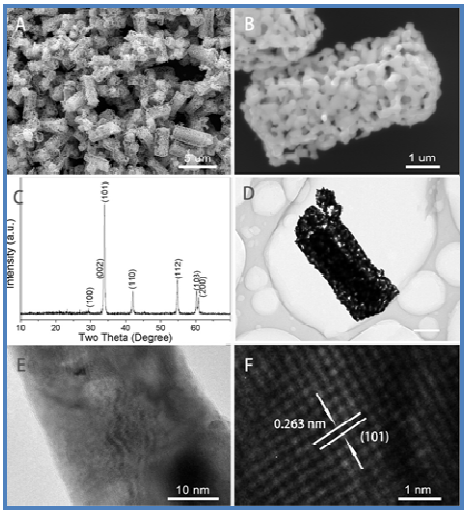

Figure 1. Structure analysis of the PoPdOMR: (A-B) SEM image; (C) XRD patterns; (D-F) TEM and HRTEM images at different magnifications.

The electrochemical test was used to investigate the effect of PoPdOMR on the catalytic activity of Cu^{2+}. Cyclic voltammograms (CVs) were recorded to understand the electrocatalytic behavior of the PoPdOMRE electrode in 0.1 M PBS solutions towards the reduction of 0.5 mM Cu^{2+} at a scan rate of 0.1 $V{\cdot}S^{-1}$. From Figure 2, two cathodic peaks are observed. Considering the standard electrode potentials and the potential-pH curves, the peak current at 0.3 V should be mainly ascribed to the oxidation of Cu to $Cu^{+}_{2}O$, as illustrated in equation (1), and the peak current at 0.5 V should be ascribed to the oxidation of $Cu^{+}_{2}O$ to Cu^{2+}, noting that all the potentials are referred to aqueous saturated calomel electrode (SCE, 0.2412V vs SHE) and the pH of the PBS solution is near 7. The catalytic mechanism of the PoPdOMRE electrode to the reduction of Cu^{2+} can be explained by the following equations (vs SHE):

$$Cu^{2+} + e^{-} \leftrightarrow Cu^{+} \quad +0.159 \quad (1)$$

$$Cu^{2+} + 2e^{-} \leftrightarrow Cu(s) \quad +0.340 \quad (2)$$

$$Cu^{+} + e^{-} \leftrightarrow Cu(s) \quad +0.520 \quad (3)$$

$$Pd^{2+} + 2e^{-} \leftrightarrow Pd(s) \quad +0.915 \quad (4)$$

With the reduction of Pd oxide, more surface-active sites are available for the reduction of both Cu^{2+} and Cu^{+}, resulting in a consecutive reduction peak. For the bulk-PdO electrode (BPdOE), its voltammetric behavior is essentially similar to that of the PoPdOMRE electrode. However, the PoPdOMRE electrode showed pronounced electrocatalytic effect for the reduction of Cu^{2+} in comparison to the BPdOE electrode. This activity is proved by the significantly enhanced peak currents for the reduction of Cu^{2+} and Cu^{+} with a reduction potential of 0.297 V, which is far less than that with the BPdOE electrode (0.402 V). However, the CVs of the PoPdOMRE electrode run in a blank PBS solution (containing no Cu^{2+}) only show reduction peaks of Pd^{2+}. The large specific surface and pore volume even results in a higher ionic current in comparison with the bulk counterpart even in the absence of copper ions. Meanwhile, almost no peak current decay was observed on the PoPdOMRE electrode after repetitive potential scan for 20 cycles at the same solutions.

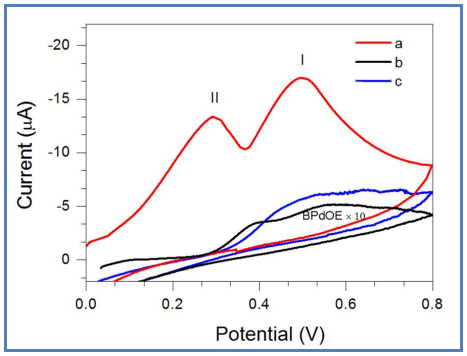

Figure 2. Cyclic voltammograms of the electrodes in 0.1 M phosphate buffer solutions (PBS, pH = 7.4) at scan rate of 0.1 $V.S^{-1}$ (a) PoPdOMRE, (b) BPdOE electrodes in the present of 10 μM Cu^{2+}, and (c) the PoPdOMRE electrode in the absence of Cu^{2+}.

A series of differential pulse voltammetry (DPV) curves were recorded at various concentrations of Cu^{2+} to determine its calibration curve. As shown in Figure 3, the response of the PoPdOMRE electrode to Cu^{2+} increases with increasing Cu^{2+} concentration suggesting that these peaks are indeed the reduction of Cu^{2+} and Cu^{+}. Inset of Figure 3A and 3B represent the two calibration curves of the PoPdOMRE electrode for the determination of Cu^{2+} based on the two cathodic peaks current, respectively. A wider linear range dependency between the current response and concentration of Cu^{2+} is observed at 300 mV (1.0×10^{-9} to 8.0×10^{-5} mM with a correlation coefficient of 0.996) than that at 510 mV (in the range of 4.0×10^{-9} - 4.0×10^{-5} mM with a correlation coefficient of 0.991). The linear dependence of current response with Cu^{2+} concentration at about 300 mV gives rise to a sensitivity of 112 μA • μM^{-1}• cm^{-2}. This phenomenon can be reasonably interpreted by the competitive adsorption model. In brief, because Cu^{2+} is reduced at about 300 mV, the products resulting from the Cu^{2+} reduction accumulated on the electrode surface during the first several additions. The accumulation of the reaction product on the electrode surface blocks some active surface sites and results in the short linear response to Cu^{2+} concentration.

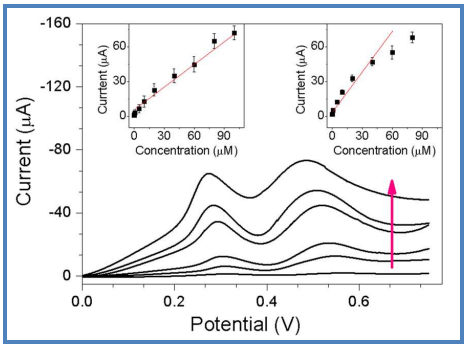

Figure 3. The DPVs of the PoPdOMRE electrode in the potential range -0.2 to 1.0 V at scan rate of 10 $mV.S^{-1}$ in 0.1M PBS (pH 7.4) solution containing Cu^{2+} at concentrations of 0.1, 1, 5, 10，20, 40, 60, and 80 μM (from bottom to top). Insets A and B are the relationship between the oxidation peak current and Cu^{2+} concentrations recorded at 300 mV and 510 mV, respectively.

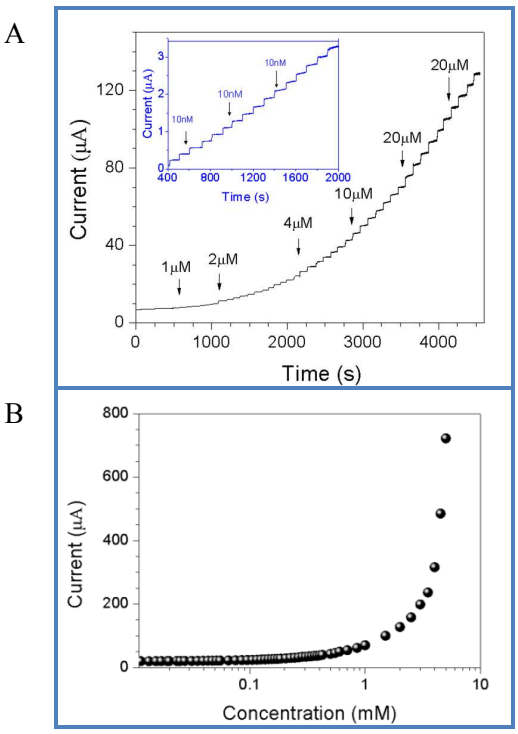

Figure 4. (A) Amperometric responses of the PoPdOMRE electrode to the successive addition of Cu^{2+} in the N_2 saturated 0.1 M PBS at 300 mV. The inset shows a close look of the response current to 10 nM Cu^{2+}. (B) Current response of the electrode to logarithm of the Cu^{2+} concentration.

This excellent catalytic activity was used to construct the sensor for detection of Cu^{2+} using chronoamperometry. Figure 4A shows the typical current-time (i-t) curves of the PoPdOMRE electrode with the successive addition of Cu^{2+} into the stirred N_2 saturated 0.1 M PBS at 300 mV since the PoPdOMRE electrode possesses wide linear range and a good sensitivity at this potential. The inset showed a close look of the response current to 10 nM Cu^{2+}. What is amazing was that the sensor was extremely sensitive to Cu^{2+} concentration at a level of nanomolar. Obvious current response could be observed with the addition of Cu^{2+} from several nanomolar to tens of millimolar for the sensor (Figure 4B), which suggested that this PoPdOMRE-based sensor could be applied to a great many systems that contain Cu^{2+} with different concentrations.

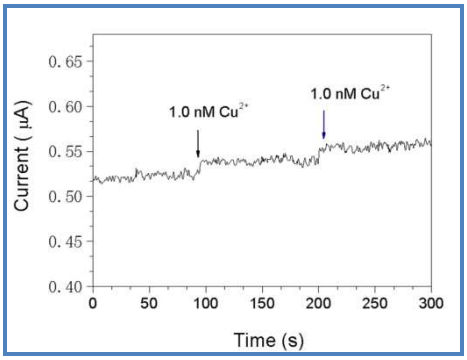

Figure 5. Determination limit of the PoPdOMRE electrode showed by the chronoamperometric curves of the PoPdOMRE electrode to successive addition of 1 nM Cu^{2+} with a constant potential at 300 mV.

The real determination limit is 1.0 nM (Figure 5). The PoPdOMRE electrode exhibits sensitive amperometric responses to Cu^{2+}, and the performance is comparable, if not superior, to those reported in other literatures (Supporting information Table 1),[3, 35-38] indicating that the PoPdOMRE electrode is very promising for analytical application.

Table 1. Comparison of different measurements for Cu2+ determination

Methods	Linear range	Detection limit
Colorimetry method [35]	2.0×10^{-5}~1.0	2.0×10^{-5}
Fluorescence spectra [36]	1.0×10^{-9}~5.0×10^{-8}	5.0×10^{-10}
Electrochemistry[37]	1.0×10^{-7}~3.0	4.6×10^{-8}
Photoelectrochemistry[38]	2.0×10^{-8}~2.0×10^{-5}	1.0×10^{-8}
Fluorescence[3]	0~9.0×10^{-4}	5.0×10^{-7}
Electrochemistry (this paper)	1.0×10^{-9}~8.0×10^{-5}	1.0×10^{-9}

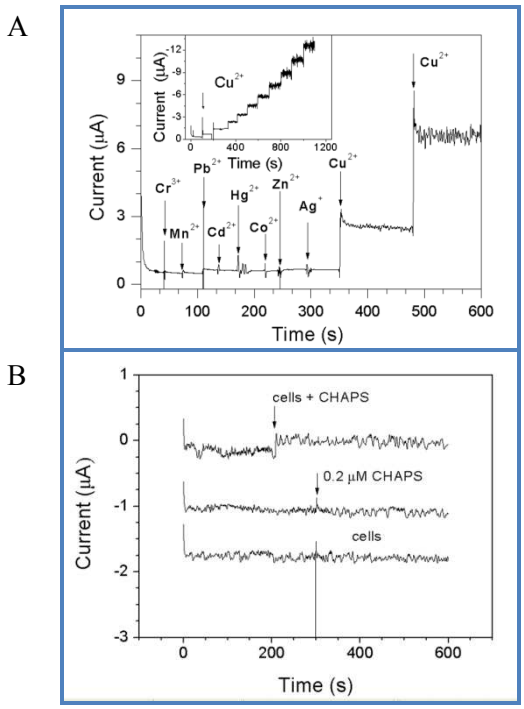

Figure 6. (A) Chronoamperometric curves of PoPdOMRE electrode in a 0.1MPBS (pH 7.4) solution with successive addition of 1 mM of Cr^{3+}, Mn^{2+}, Pb^{2+}, Cd^{2+}, Hg^{2+}, Co^{2+}, Zn^{2+}, Ag^{+} with a constant potential at 300 mV. Inset is the corresponding chronoamperometric curves of the PoPdOMRE electrode to successive addition of 1 μM Cu^{2+} without addition any interfering species in the same conditions. (B) Amperometric responses of the PoPdOMRE electrode to the addition of 0.3 μM CHAPS with, without Raw 264.7 cells, as well as in the presence of Raw 264.7 cells without CHAPS in the N_2 saturated 0.1 M PBS at 300 mV.

An important parameter for a sensor is its ability to discriminate between these competitive ions commonly present in similar environment and the target analyte. We further investigate the amperometric detection of Cu^{2+} at 300 mV on the PoPdOMRE electrode to determine the selectivity for Cu^{2+}

sensing. Figure 6A presents the testing results on selectivity of the PoPdOMRE electrode with successive additions of Cr^{3+}, Mn^{2+}, Pb^{2+}, Cd^{2+}, Hg^{2+}, Co^{2+}, Zn^{2+}, Ag^{+} (the general competitive cation encountered in environmental and biological analyses) in 0.1M PBS solution. Interestingly, the PoPdOMRE electrode produces negligible current signals for all eight common interfering ions, yet still gives out significant responses to incremental Cu^{2+} concentrations. However, taking the amperometric responses of the PoPdOMRE electrode to successive addition of 1μM Cu^{2+} without interferences for comparison, there has a 3% decrease in sensitivity of each current response of the added Cu^{2+} with the presence of the competitive ions, the system is useful for selectively sensing Cu^{2+} even involving these relevant cations. The constructed sensor was then used for the real-time tracking of Cu^{2+} released by Raw 264.7 cells due to its low determination limit, good reproducibility, and selectivity. 3-[(3-Cholamidopropyl) dimethylammonio]-1-propanesulfonate (CHAPS) was used to stimulate the cells to generate Cu^{2+}. Around 2×10^{6} cells were re-suspended in 20 mL of PBS (pH = 7.4) for electrochemical measurement. After treated with 0.3 μM CHAPS, an obvious current change that corresponding to 20 nM Cu^{2+} could be observed, while no signal could be observed if cells were not treated with CHAPS (Figure 6B).

For environmental and biological applications of the electrochemical sensor, we also investigated the suitable pH range for Cu^{2+} sensing on the PoPdOMRE electrode. Figure 7 shows the dependences of the Cu^{2+} peak current response on the buffer solution pH in 0.1 M PBS solution containing 10 μM Cu^{2+}. The cathodic peak current increased with increasing solution pH, while peaked at pH 7.0. When the solution pH was above 7.0, the peak current response decreased. This might be due to the formation of $Cu(OH)_2$. As electrocatalytic signal was sufficient for detection in PBS of physiological condition (pH 7.4) which is the most commonly used and environment-friendly, pH 7.4 was selected for detection solution.

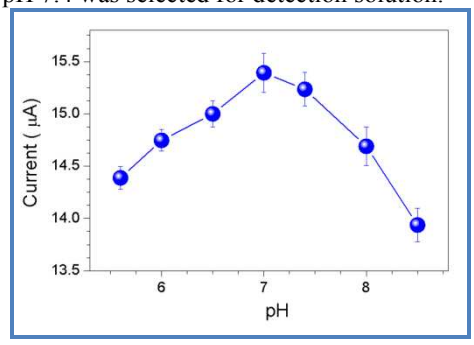

Figure 7 . Relationship between solution pH and the reduction peak current at the PoPdOMRE electrode. The concentration of Cu^{2+} is 10 μM.

The operational stability of the PoPdOMRE electrode is tested by monitoring the current response after 100 successive measurements (Figure 8). It can be seen that the peak current intensity remains 96.2% of its initial value. The storage stability is examined at the same modified electrode in consecutive 30 days. While not in use, the modified electrode is stored in air. In the repeated measurements in consecutive days, the response to the reduction of the same concentration of Cu^{2+} at the optimum potential is maintained 98% of the initial values. The good long-term stability could be attributed to both the structural stability and good adsorption of the porous PdO microrods on the surface of GCE electrode.

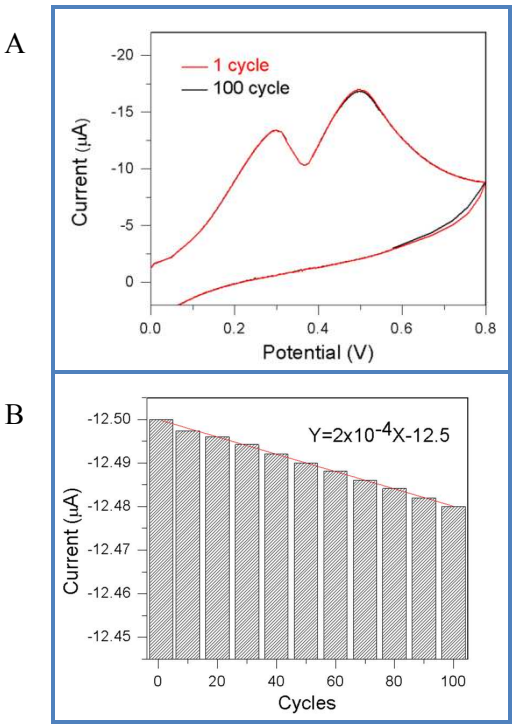

Figure 8. CVs of PoPdOMRE electrode in 0.5 mM Cu^{2+} PBS solutions for the first and the 100th cycles. Potential range: 0 to 0.8 V, scan rate: $0.1V\bullet s^{-1}$. (B) A plot of the peak current with the cycling number.

4. Conclusions

In summary, porous PdO microrods have been conveniently synthesized through a simple solution chemical process. Due to the porous structure, high specific surface areas, the as fabricated PoPdOMRE electrode shows an excellent electrocatalytic activity toward the reduction on of Cu^{2+} and could be used for the detection of the trace amount of Cu^{2+} released by the cells. It is also interesting to note that the competitive cation could be successfully avoided and a good selectivity toward the sensing of Cu^{2+} was obtained. In addition, the PoPdOMRE electrode shows outstanding mechanical and chemical stability, which makes it promising for mass production of the sensors at low cost and on a large scale.

Acknowledgement

We thank the financial support from the National Natural Science Foundation of China (NSFC No. 21275102, 21173017, and 21075004), The Program for New Century Excellent Talents in University (NCET-12-0610), The science and technology research projects from education ministry (213002A), National "Twelfth Five-Year" Plan for Science & Technology Support (No.2011BAZ01B06), Project of Thousand Talents of Chinese High-leveled Talents and the Knowledge Innovation Program of the Chinese Academy of Science (Grant No. KJCX2-YW-M13)

Notes and references

[a] Beijing Institute of Nanoenergy and Nanosystem, Chinese Academy of Science, Beijing, 100083, China;

[b] Key Laboratory of Bio-Inspired Smart Interfacial Science and Technology of Ministry of Education, School of Chemistry and Environment, Beijing University of Aeronautics and Astronautics, Beijing, 100083, China;
[c] School of Biochemical and Pharmaceutical Sciences, Capital Medical University, Beijing, 100069, China
* To whom all correspondence should be addressed. E-mail: caoxia@binn.cas.cn (X.C.), wangning@buaa.edu.cn (N.W.).

1. A. Afkhami, F. Soltani-Felehgari, T. Madrakian, H. Ghaedi and M. Rezaeivala, *Anal Chim Acta*, 2013, 771, 21-30.
2. H. Ahn, S. Y. Kim, O. Kim, I. Choi, C. H. Lee, J. H. Shim and M. J. Park, *Acs Nano*, 2013, 7, 6162-6169.
3. R. O. Allen and Brookhar.W, *Anal Chem*, 1974, 46, 1297-1299.
4. X. Y. Qiu, S. H. Han and M. Gao, *J Mater Chem A*, 2013, 1, 1319-1325.
5. L. Cui, J. Wu, J. Li, Y. Q. Ge and H. X. Ju, *Biosens Bioelectron*, 2014, 55, 272-277.
6. M. L. Wang, G. W. Meng, Q. Huang and Y. W. Qian, *Environ Sci Technol*, 2012, 46, 367-373.
7. Q. T. Meng, X. L. Zhang, C. He, G. J. He, P. Zhou and C. Y. Duan, *Adv Funct Mater*, 2010, 20, 1903-1909.
8. J. Otero-Romani, A. Moreda-Pineiro, A. Bermejo-Barrera and P. Bermejo-Barrera, *Anal Chim Acta*, 2005, 536, 213-218.
9. W. W. Xiong, G. H. Yang, X. C. Wu and J. J. Zhu, *J Mater Chem B*, 2013, 1, 4160-4165.
10. J. Zhang, B. Li, L. M. Zhang and H. Jiang, *Chem Commun*, 2012, 48, 4860-4862.
11. Y. Kong, J. Li, S. Wu, W. Cheng, R. K. Rana and J. J. Zhu, *Sensor Actuat B-Chem*, 2013, 183, 187-193.
12. H. P. Huang, G. F. Jie, R. J. Cui and J. J. Zhu, *Electrochem Commun*, 2009, 11, 816-818.
13. D. P. Tang, B. Zhang, B. Q. Liu, G. N. Chen and M. H. Lu, *Biosens Bioelectron*, 2014, 55, 255-258.
14. Z. Dai, S. Serban, H. X. Ju and N. El Murr, *Biosens Bioelectron*, 2007, 22, 1700-1706.
15. Y. L. Liu, X. Lv, Y. Zhao, J. Liu, Y. Q. Sun, P. Wang and W. Guo, *J Mater Chem*, 2012, 22, 1747-1750.
16. D. W. Pan, Y. E. Wang, Z. P. Chen, T. T. Lou and W. Qin, *Anal Chem*, 2009, 81, 5088-5094.
17. X. X. Xu, S. Q. Liu and H. X. Ju, *Sensors*, 2003, 3, 350-360.
18. Y. Q. Han, Y. Wu, M. X. Shen, X. L. Huang, J. J. Zhu and X. G. Zhang, *J Mater Sci*, 2013, 48, 4214-4222.
19. S. Y. Ma, L. Liu, V. Bromberg and T. J. Singler, *J Mater Chem C*, 2014, 2, 3885-3889.
20. S. Tang and M. S. Dresselhaus, *J Mater Chem C*, 2014, 2, 4710-4726.
21. Y. F. Wu, C. L. Chen and S. Q. Liu, *Anal Chem*, 2009, 81, 1600-1607.
22. B. Mondal, P. Kumar, P. Ghosh and A. Kalita, *Chem Commun*, 2011, 47, 2964-2966.
23. B. Q. Liu, D. P. Tang, J. Tang, B. L. Su, Q. F. Li and G. N. Chen, *Analyst*, 2011, 136, 2218-2220.
24. C. M. Deng, Y. Y. Geng and Y. Q. Wu, *J Mater Chem C*, 2013, 1, 2470-2476.
25. J. Cookson, *Platinum Metals Rev*, 2012, 56, 83-98.
26. A. X. Yin, X. Q. Min, W. Zhu, W. C. Liu, Y. W. Zhang and C. H. Yan, *Chem-Eur J*, 2012, 18, 777-782.
27. P. A. Szilagyi, R. J. Westerwaal, R. van de Krol, H. Geerlings and B. Dam, *J Mater Chem C*, 2013, 1, 8146-8155.
28. H. Cheng and K. Scott, *Appl Catal B Environ*, 2011, 108–109, 140-151.
29. J. Sunarso, A. M. Glushenkov, A. A. J. Torriero, P. C. Howlett, Y. Chen, D. R. MacFarlane and M. Forsyth, *J. Electrochem. Soc.*, 2013, 160, H74-H79.
30. C.-S. Chen and F.-M. Pan, *J. Power Sources*, 2012, 208, 9-17.
31. J.-J. Feng, D.-L. Zhou, H.-X. Xi, J.-R. Chen and A.-J. Wang, *Nanoscale*, 2013, 5, 6754-6757.
32. G. Groppi, C. Cristiani, L. Lietti and P. Forzatti, in *Stud. Surf. Sci. Catal.*, eds. F. V. M. S. M. Avelino Corma and G. F. José Luis, Elsevier, 2000, vol. Volume 130, pp. 3801-3806.
33. A. L. Isfahani, I. Mohammadpoor-Baltork, V. Mirkhani, A. R. Khosropour, M. Moghadam, S. Tangestaninejad and R. Kia, *Appl Catal B Environ*, 2013, 355, 957-972.
34. V. Chandrasekhar, S. Das, R. Yadav, S. Hossain, R. Parihar, G. Subramaniam and P. Sen, *Inorg Chem*, 2012, 51, 8664-8666.
35. X. Y. Xu, W. L. Daniel, W. Wei and C. A. Mirkin, *Small*, 2010, 6, 623-626.
36. C. S. Wu, M. K. K. Oo and X. D. Fan, *Acs Nano*, 2010, 4, 5897-5904.
37. M. Lin, X. K. Hu, Z. H. Ma and L. X. Chen, *Anal Chim Acta*, 2012, 746, 63-69.
38. G. L. Wang, J. J. Xu and H. Y. Chen, *Nanoscale*, 2010, 2, 1112-1114.

